HHS Public Access

Author manuscript

Osteoarthritis Cartilage. Author manuscript; available in PMC 2022 November 01.

Published in final edited form as:

Osteoarthritis Cartilage. 2021 November ; 29(11): 1549–1563. doi:10.1016/j.joca.2021.08.008.

Effects of Long-Term Exercise and a High-Fat Diet on Synovial Fluid Metabolomics and Joint Structural Phenotypes in Mice: An Integrated Network Analysis

Alyssa K. Hahn, PhD[1,2,3,#], **Albert Batushansky, PhD**[4,#], **Rachel A. Rawle, PhD**[1,5], **Erika Barboza Prado Lopes, PhD**[4], **Ronald K. June, PhD**[1,2,6,*], **Timothy M. Griffin, PhD**[4,7,8,*]

[1]Molecular Biosciences Program, Montana State University, Bozeman, MT, USA, 59717.

[2]Department of Cell Biology & Neuroscience, Montana State University, Bozeman, MT, USA, 59717.

[3]Department of Biological and Environmental Sciences, Carroll College, Helena, MT, USA, 59625.

[4]Aging and Metabolism Research Program, Oklahoma Medical Research Foundation (OMRF), Oklahoma City, OK, USA, 73104.

[5]Department of Microbiology & Immunology, Montana State University, Bozeman, MT, USA, 59717.

[6]Department of Mechanical & Industrial Engineering, Montana State University, Bozeman, USA.

[7]Reynolds Oklahoma Center on Aging, Department of Biochemistry and Molecular Biology, Department of Physiology, University of Oklahoma Health Sciences Center, Oklahoma City, OK, USA, 73104.

[8]Veterans Affairs Medical Center, Oklahoma City, OK, USA, 73104.

Abstract

Objective: To explore how systemic factors that modify knee osteoarthritis risk are connected to ‘whole-joint’ structural changes by evaluating the effects of high-fat diet and wheel running exercise on synovial fluid (SF) metabolomics.

[*]Co-corresponding authors Ronald K. June, Ph.D., Dept. of Mechanical & Industrial Engineering, Montana State University, PO Box 173800, Bozeman, MT 59717-3800, Phone: (406) 994-5941; Fax: (406) 994-6292, rjune@montana.edu; Timothy M. Griffin, Ph.D., Aging and Metabolism Research Program, Oklahoma Medical Research Foundation, MS 21, 825 NE 13th St, Oklahoma City, OK 73104 USA, Phone: (405) 271-7579; Fax: (405) 271-1437; Tim-Griffin@omrf.org.

[#]Authors contributed equally to this work

Author contributions

All authors contributed to either the study design (ALK, AB, RKJ, TMG), acquisition of data (AKH, RAR, EBPL, TMG), or analysis and interpretation of data (AKH, AB, RAR, RKJ, and TMG). AKH, RKJ, and TMG drafted the article, and all authors revised it critically for intellectual content. All authors approved the final version to be published.

Competing Interests

The authors declare no competing interests.

Methods: Male mice were fed a defined control or high-fat (60% kcal fat) diet from 6 to 52 weeks of age, and half the animals were housed with running wheels from 26 to 52 weeks of age (n=9-13 per group). Joint tissue structure and osteoarthritis pathology were evaluated by histology and micro-computed tomography. Systemic metabolic and inflammatory changes were evaluated by body composition, glucose tolerance testing, and serum biomarkers. SF metabolites were analyzed by high performance-liquid chromatography mass spectrometry. We built correlation-based network models to evaluate the connectivity between systemic and local metabolic biomarkers and osteoarthritis structural pathology within each experimental group.

Results: High-fat diet caused moderate osteoarthritis, including cartilage pathology, synovitis and increased subchondral bone density. In contrast, voluntary exercise had a negligible effect on these joint structure components. 1,412 SF metabolite features were detected, with high-fat sedentary mice being the most distinct. Diet and activity uniquely altered SF metabolites attributed to amino acids, lipids, and steroids. Notably, high-fat diet increased network connections to systemic biomarkers such as interleukin-1β and glucose intolerance. In contrast, exercise increased local joint-level network connections, especially among subchondral bone features and SF metabolites.

Conclusion: Network mapping showed that obesity strengthened SF metabolite links to blood glucose and inflammation, whereas exercise strengthened SF metabolite links to subchondral bone structure.

Keywords

Osteoarthritis; Obesity; Exercise; Metabolomics; Synovial Fluid; Systems Biology

Introduction

The development of effective disease-modifying osteoarthritis (OA) drugs is hampered by the chronic, multi-factorial nature of OA pathogenesis. To tackle this complexity, recent perspectives have highlighted the need for systems-based approaches in OA studies[1,2]. This includes an expansion from cartilage-centric studies to ‘whole-joint’ analyses[3] and consideration of whole-body systemic factors in OA, especially in the context of obesity, metabolic syndrome, and inflammation[4-6]. One strategy for exploring complex interactions in OA pathophysiology is by developing data-driven network inference models, which often include “omic” data to infer causality or association for future hypothesis testing.

Metabolomics is a promising approach for understanding the relationship between systemic and local factors in OA[7-9]. Metabolomics involves the analysis of small molecules to broadly evaluate changes in cellular metabolism across tissues and organ systems[10]. Metabolomic-based analyses discriminate between healthy and OA patients when applied to synovial fluid (SF)[11-14], synovium[15], serum[16,17], and urine[18]. In addition, comparisons of SF metabolites from early and late-stage OA reveal numerous differences[19,20], suggesting that metabolites may serve as biomarkers of disease severity. Although many metabolites are readily detected in serum, <5% of serum metabolites were significantly correlated with SF levels in a paired analysis[21]. Thus, the SF metabolome may better reflect proximal factors involved in OA pathogenesis and disease progression.

The objective of this study was to determine how obesity and exercise – two systemic factors that modify OA risk[22,23] – affect the SF metabolome and to explore the relationship with 'whole-joint' structural changes using network correlation analysis. Mouse models of high-fat (HF) diet-induced obesity are widely used to study the molecular mechanisms of metabolic inflammation associated with the pathogenesis of metabolic syndrome and related metabolic diseases[24,25]. We previously established the utility of this model for studying obesity-associated knee OA[26-29]. We also showed that voluntary exercise in young adult mice fed a high-fat diet protected against early knee OA despite no reduction in body mass, body fat, or serum inflammatory cytokines[27]. These findings suggest that exercise protects against OA by altering local mediators of joint homeostasis.

In the current study, we evaluated the effects of long-term HF diet and voluntary wheel running exercise on systemic metabolic and inflammatory factors, joint structure, and SF metabolites in mice. These initial results were evaluated using standard analyses of group means. We then integrated this comprehensive set of phenotypic outcome data by constructing correlation-based network models for each diet and activity group. We hypothesized that SF metabolomic profiling would reveal distinct effects of HF diet and exercise on metabolic pathways related to changes in joint tissue structure and OA pathology. We tested this exploratory hypothesis by quantitatively comparing the correlation network models across each of the four diet and physical activity conditions.

Materials and Methods

Animals, Treatments, and Phenotyping

All experiments were conducted following approval by the AAALAC-accredited IACUC at the Oklahoma Medical Research Foundation. Male C57BL/6J mice were purchased from The Jackson Laboratory (USA) through the Diet-Induced Obese Mouse service, which assigns animals to one of two irradiated, purified open source diets (Research Diets Inc., USA) beginning at 6 weeks of age: 1) control-fat diet (CF) containing 10% kcal fat (D12450Bi), or 2) high-fat diet (HF) containing 60% kcal fat (D12492i). 24 CF and 26 HF fed animals were delivered to OMRF at 20-21 wks of age and maintained on their respective diets. Ages were staggered so that behavioral and metabolic tests could be conducted on aged-matched animals. At 26 wks of age, 12 CF and 12 HF mice were assigned to the exercise treatment group, which involved single-housing with running wheels as previously described[30]. Individual animals were assigned to the exercise group so that the distribution and average body mass of animals were similar to those in their diet-matched sedentary cohort. Following activity assignments, all animals (including sedentary) were single-housed for the remainder of the study. Animals underwent various metabolic, functional, and imaging tests over the course of the study (Fig. 1). Mice were euthanized at 52 wks of age by rapid decapitation using a guillotine device to minimize tissue metabolic alterations caused by exposure to carbon dioxide or anesthesia agents. Additional details are provided in the Supplemental Methods.

Serum Analysis

Serum was aliquoted and frozen at −80°C until analysis. Samples were shipped on dry ice to Dr. Virginia Kraus's laboratory at Duke University for analysis. Concentrations of IFN-γ, IL-1β, IL-6, IL-10, IL12p70, IL-8 (KC), and TNF-α were measured using the Mouse Pro-inflammatory Ultra-Sensitive sandwich immunoassay 7-plex kit (#K15012C, MSD, USA). Serum concentrations of adiponectin (#K0013182, MSD), IGF-1 (#MG100, R&D, USA), leptin (#MOB00, R&D), CCL2, also known as MCP-1, (#MJE00, R&D), and VCAM-1 (#MVC00, R&D) were measured following manufacturer instructions. Serum dilutions, lowest levels of detection, intra-assay coefficients of variation, and additional details are provided in the Supplemental Methods.

Joint Structural Analysis

High-resolution micro-computed tomography (CT) scanning was performed on the right knee using a vivaCT 40 scanner (Scanco Medical, Basserdorf, Switzerland) following prior protocols[30]. Subchondral bone and proximal tibial epiphyseal trabecular bone density and morphology were evaluated as previously described[31]. The right knee was then processed and prepared for histological grading[28]. Two experienced graders evaluated multiple stained sections from the medial and lateral joint compartments. Slides were organized by animal, randomized by treatment, and assigned a temporary identification code to blind graders to group assignment. Each grader independently assigned Modified Mankin OA scores separately for the medial/lateral femur and tibia, with a maximal site-specific score of 24. Osteophyte severity and synovial pathology were evaluated as recently described[29]. Modified Mankin OA outcomes were previously reported for sedentary CF and HF animals[28]. Additional details are provided in Supplemental Methods.

Synovial Fluid Metabolomics

SF was collected from the left knee immediately following death using the calcium sodium alginate compound method[32] and maintained at −80°C until analysis. Samples were shipped on dry ice to the June Laboratory for further processing. A pilot study confirmed the feasibility of mouse SF metabolomic analyses (Fig. S1). Proteins were precipitated with acetone, and metabolites were extracted using 50:50 water:acetonitrile following previously established protocols[11]. Metabolite extracts were analyzed in positive mode using an Agilent 1290 UPLC system connected to an Agilent 6538 Q-TOF mass spectrometer (Agilent Santa Clara, CA). Mass spectra were then processed using MZMine 2.14 for peak detection, noise threshold (1000), retention time and mass-to-charge (m/z) ratio normalization, and alignment of peaks[33]. For quality control, a pooled sample analyzed three times over the span of 24 hours showed a mean coefficient of variation (CV) value of 11.9 and median CV of 8.0 for 573 features. Metabolite features were defined based on all detected m/z values and corresponding relative abundance of each m/z value. Additional details are provided in Supplemental Methods.

Data Analytics and Statistics

Pre-exercise diet treatment effects on body composition, glucose intolerance and gait biomechanics were analyzed by two-tailed Student's t-test. The effects of diet and exercise

treatments on systemic metabolic and inflammatory related outcomes and joint structural outcomes were evaluated by two-way ANOVA (Prism 8.4.3 for Mac OS X) (Table S1). Tidemark scoring and serum data did not meet assumptions for homoscedasticity or normality of residuals and were therefore log-transformed. Tests showing a significant effect of diet, exercise, or interaction effects ($p<0.05$) were followed up with multiple-comparison post-hoc tests to identify individual group differences as specified in figure legends. For SF metabolomic analyses, metabolite features with a median intensity of zero across all experimental groups were removed from the analysis. Remaining intensity values of zeroes were considered below the detection limit and thus replaced with one-half the minimum intensity value identified in the dataset[34]. Statistical analyses were completed in MATLAB (Mathworks, Inc.) and MetaboAnalyst[34]. Metabolite features were matched to metabolite identities using the KEGG database in MS Peaks to Pathways in MetaboAnalyst[35]. Implicated pathways were determined using MS Peaks to Pathways in MetaboAnalyst utilizing Mummichog[34,36]. Relevant pathways were identified by *a priori* FDR-corrected significance levels of $q_{FDR}=0.05$ using the KEGG database. Sample size justification and sample processing procedures are described in detail in Supplemental Methods.

Correlation Network Analysis

Correlation-based networks were constructed for each diet and physical activity condition separately using established methods[37]. Data sets for joint structure outcomes (24 variables), systemic metabolic and inflammatory outcomes (19 variables), and SF metabolite levels (264 variables) (Table S3) were obtained for 9 animals per group and integrated using diet- and activity-specific Pearson's correlation matrices calculated for each group using the R "psych" package[38]. For groups with >9 animals, nine were randomly selected to maintain equal degrees of freedom across all networks. Only correlation coefficients with $r>|\pm0.5|$ and $q_{FDR}<0.05$ were considered for network construction. The q_{FDR} criterion resulted in a minimum correlation coefficient of $r>|\pm0.7|$. Networks were visualized in Cytoscape[39]. Graph theory-based network properties and odds ratio analyses were calculated in R using "iGraph"[40] and built-in functions, respectively. Odds ratios (OR) were calculated to estimate the likelihood of associations (observed versus expected) occurring between joint structural parameters and synovial fluid metabolites relative to associations between joint structural parameters and systemic factors. Dijkstra's algorithm identified nodes contributing the shortest path in each network linking body weight to the whole-joint OA score. The r-value was used as the edge weight, which was then transformed to a distance matrix for Dijkstra's algorithm. Additional methods are described in Supplemental Methods.

Results

Effect of HF diet and wheel running on systemic metabolic and inflammation outcomes

Prior to initiating the exercise phase of the study, HF diet mice developed greater body mass (6.8 g [4.5, 9.1]; mean difference [95% CI of difference]) and showed mild glucose intolerance (Fig. S2). On average, HF animals ran significantly shorter distances and durations per day than CF animals (4.5 km less per day [3.5, 5.4] and 153 min less per day [121, 185]), especially as animals aged (Fig. S3A,B). An exploratory analysis of wheel running biomechanics in a subset of animals showed that HF animals ran slower with

longer hindfoot contact times. Absolute peak hindlimb forces were 33% greater in HF mice; however, peak normal and propulsive forces were lower in HF animals when normalized to body weight (Fig. S3C-E).

At study end, body mass and body fat remained substantially elevated in HF mice regardless of activity (Fig. 2A). Exercise led to a modest reduction in body mass, body fat, and gonadal fat pad mass in CF but not HF animals (Fig. 2A). In contrast to the pre-exercise test, fasting blood glucose and glucose tolerance were not altered by a HF diet alone at one year of age and were modestly reduced by exercise in CF versus HF mice (Fig. 2B). Gonadal fat stromal vascular fraction immune cells ($CD45^+$ cells) were evaluated in a subset of animals (Fig. 2C), with exercise reducing $CD45^+$ immune cells in CF but not HF mice. As with prior studies[28], a HF diet increased the relative number of pro-inflammatory adipose tissue myeloid cells ($F4/80^+CD11c^+$), which was partially reduced by exercise in HF mice (Fig. 2C). At the systemic level, the effect of exercise on serum inflammatory mediators was modest compared to a HF diet. HF feeding increased serum leptin, IL-8, CCL2, and IL-10 (Fig. 2D). Exercise reduced serum leptin levels in CF mice and normalized the concentration of IL-10 between CF and HF animals (Fig. 2D). Other metabolic and inflammatory mediators (i.e., adiponectin, IGF-1, IL-6, IL-1β, VCAM-1, and IL-12p70) were not altered by HF diet or exercise (Fig.2D, Fig. S4).

Minimal effect of wheel running on HF diet-induced OA outcomes and joint structure

A HF diet significantly increased the modified Mankin OA score (1.6 [0.7, 2.5]; mean difference [95% CI of difference]; p=0.0005, 2-way ANOVA) (Fig. 3A). Exercise did not alter the OA score (p=0.93) or interact with diet (p=0.87). The increased OA score in HF diet mice was due to an increase in cartilage structural damage and loss of Safranin-O staining (Fig. 3A,C). Exercise reduced hypertrophic chondrocytes in the calcified cartilage in CF but not HF mice (Fig. 3A). Neither HF diet nor exercise altered cartilage tidemark number. HF diet did not increase the severity of anterior-posterior osteophytes (Fig. 3A) despite observing this effect at an earlier timepoint[28]. Although the effect of exercise on osteophyte severity was inconclusive, the average score was reduced with exercise irrespective of diet (−0.37 [0.002, −0.74]; p=0.051, 2-way ANOVA). Mild synovitis was detected in animals fed a HF diet, with an increase in the maximal synovial lining cell number in sedentary animals (+1.0 cells [0.35, 1.7]; p=0.004) and possible synovial thickening (9.7 μm [−0.5, 19.8]; p=0.06) (Fig. 3B). Neither HF diet nor exercise altered IFP mass, a potential mediator of joint inflammation (Fig. 3B). Taken together, these results indicate that long-term HF diet induced moderate OA pathology. The results also show that voluntary wheel running exercise had minimal impact on knee OA, independent of diet.

Subchondral cortical and trabecular bone were also evaluated for OA-related joint structure changes. A HF diet increased subchondral cortical bone mineral density in the medial tibial plateau (33.2 mg HA/cm^3 [14.1, 52.2]; p=0.001, 2-way ANOVA) (Fig. 4A). A HF diet also increased the trabecular bone mineral density in sedentary mice (p=0.01), but exercise blocked this effect (Fig. 4A). The most substantial effect of HF diet and exercise was on trabecular connectivity density, which was reduced by a HF diet and by exercise in CF animals (Fig. 4B; 2-way ANOVA: diet, p=0.002; activity, p=0.69, interaction, p=0.01).

This reduction in connectivity density was associated with a possible, but inconclusive, increase in trabecular thickness in sedentary HF animals but not in exercising animals (2-way ANOVA: interaction, p=0.06).

HF diet and wheel running induce distinct SF metabolomes

A total of 1,412 features were detected in the knee joint SF (Fig. 5A). Hierarchical cluster analysis of median metabolite profiles showed the most distinct metabolomic profile in HF sedentary mice (Fig 5A). In contrast, HF exercise mice had SF metabolomic profiles most similar to CF sedentary mice. Cluster-based pathway analyses revealed distinct effects of diet and exercise on SF metabolite classes. For example, exercise downregulated metabolites involved in fatty acid metabolism, steroid biosynthesis, pyruvate metabolism, tryptophan metabolism, and lysine degradation (e.g., clusters 3 and 7, Fig. 5B). In contrast, SF metabolites from HF sedentary mice were positively associated with short-chain fatty acids, coenzyme-A biosynthesis, and branched chain amino acid degradation (e.g., cluster 4, Fig. 5B). A full enrichment analysis of clusters, including specific metabolite features and non-significant pathways, is included in Table S2.

The effects of diet and exercise on specific SF metabolite features were further evaluated by volcano plots (Fig. 6). In sedentary cohorts, HF diet downregulated 15 metabolite features and did not upregulate any metabolite features in comparison to CF diet mice (Fig. 6A). In contrast, in exercise cohorts, a HF diet upregulated 18 metabolite features and downregulated 8 features in comparison to CF diet mice (Fig. 6B). When HF diet comparisons were based on more stringent criteria (Fig. 6C), all altered features were unique to either sedentary or exercise cohorts except for one, whose predicted annotation was alpha-Tocotrienoxyl radical. A complementary approach was taken to evaluate mechanosensitive SF metabolites. In CF mice, exercise increased 12 metabolite features and lowered 25 (Fig. 6D); whereas, in HF diet cohorts, exercise increased 11 metabolite features and lowered 3 (Fig. 6E). When exercise comparisons were based on more stringent criteria (Fig. 6F), all but one feature were unique to either CF or HF diet cohorts. The feature present in both cohorts, which is predicted to be an alpha-Tocotrienoxyl radical, appears to have a diet-specific response to exercise, being reduced by exercise in CF mice and increased in HF mice. However, this interaction effect requires a 2-factor analysis to confirm.

Correlation-based network analysis reveals integrative response to diet and exercise

Correlation-based networks were generated for each of the four unique diet and physical activity cohorts by integrating systems-level metabolic and inflammatory biomarkers, subchondral bone and OA pathology data, and SF metabolite features (Table S1). All networks had similar global properties and a high tendency to form modules based mainly on many positively correlated pairs of SF metabolite features being the same across networks (Table S2, Fig. S5). However, exercise had diet-specific effects on the network diameter and percent negative correlations (Table S2). These differences were due to 10-15% of the correlated pairs of variables, including all negatively correlated pairs, being unique to each diet and activity condition.

These unique network correlations primarily occurred between variables belonging to different phenotype sub-groups (i.e., systemic factors, joint structure, or SF metabolites). Consequently, we summarized the number of vertices (i.e., variables with ≥1 correlation) within each sub-group to a single node and compared the number of edges (i.e., paired correlations) across each sub-group node for each diet and physical activity group (Fig. 7). We statistically evaluated these comparisons by calculating the odds ratios (OR) of observed versus expected edges between sub-group nodes for each diet and activity condition. In the CF-sedentary condition, the number of observed correlated pairs (i.e., the "connectivity") between joint structure and SF metabolites versus joint structure and systematic factors favored systemic factors such that the OR was significantly less than one (OR: 0.25 [0.13, 0.49] [95% CI]). Under the HF-sedentary condition, the connectivity similarly favored joint structure and systematic factors (OR: 0.16 [0.05, 0.56]). In contrast, connectivity between SF metabolites and joint structure was greatly elevated in the CF-exercise condition relative to systemic factors (OR: 6.21 [2.38, 23.0]). Connectivity between SF metabolites and joint structure features was also enhanced in the HF-exercise group relative to HF-sedentary, although the effect was much smaller than in CF-exercise animals such that connectivity between joint structure and systematic factors remained dominant (OR: 0.45 [0.24, 0.92]).

We next extracted the network modules that primarily contributed to these diet and activity differences. The dominant CF-sedentary network occurred through two linked vertices with positive connections to SF metabolites: medial tibia subchondral bone mineral density and serum vascular cell adhesion molecule-1 (VCAM-1). Notably, diacylglycerols and triacylglycerols were among the positively correlated SF metabolites (Fig. 7). Under HF-sedentary conditions, joint structure connectivity shifted further towards systemic factors and included increased connectivity between SF metabolites and systemic factors. In particular, glucose intolerance (i.e., serum glucose area-under-the-curve following a GTT test) and serum insulin-like growth factor 1 (IGF-1) were negatively correlated with multiple SF metabolites, including phosphatidylglycerols and phosphatidylcholines (Fig. 7). Conversely, serum interleukin-1β and infrapatellar fat pad mass were positively correlated with one-another and with numerous classes of SF metabolites (Fig. 7). In the CF-exercise condition, a high increase in connectivity between joint structure and SF metabolites occurred largely through two joint structure bone features: medial tibial subchondral bone mineral density and tibial epiphysis bone volume to tissue volume (BV/TV). These two vertices shared a large number of SF metabolite links, including branched chain amino acids and short chain fatty acids (Fig. 7). The HF-exercise network also strengthened connectivity to joint structure variables, such as re-establishing the module linking medial tibia subchondral bone mineral density and SF metabolites. However, connectivity between SF metabolites and systemic factors remained high, albeit with a shift to fasting blood glucose and serum IL-10 (Fig. 7).

Finally, to gain insight into network factors associated with knee OA, we used Dijkstra's algorithm to determine the variables connecting body weight to the modified Mankin knee OA score. The results demonstrated a consistent involvement of SF metabolites into the establishment of this shortest path in all groups except the CF sedentary group. Many of these SF metabolites were tentatively identified as involved in extracellular lipid transport (Fig. 8). Altogether, these results support a reprograming of local metabolism in the joint

with respect to diet and physical activity level that underlies the relationship between body weight and OA pathology.

Discussion

We examined how systemic factors that modify OA risk affect the SF metabolome. Notably, HF sedentary mice had the most unique profile of SF metabolites, characterized by short-chain fatty acids, coenzyme-A biosynthesis, and branched chain amino acid degradation. We then integrated systemic and local phenotypic data using a correlation network analysis to identify metabolic pathways related to 'whole-joint' knee structural changes. Network analyses provide powerful quantitative frameworks for integrating complex data, which we recently illustrated in a separate study of murine OA phenotypes[30]. We hypothesized that SF metabolomic profiling would reveal how a HF diet and exercise alter metabolic pathways associated with specific joint tissue structural changes.

Our findings support this hypothesis, revealing both shared and distinct network modules involving systemic biomarkers, joint structure features, and SF metabolites across diet and activity conditions. HF sedentary mice were distinguished by strong links between SF metabolites and systemic metabolism related to IFP mass, serum IL-1β, glucose intolerance, and serum IGF-1. However, in HF exercise mice, the link to pro-inflammatory mediators was broken and a network involving subchondral bone mineral density and SF metabolites was re-established as observed in the CF cohorts. The impact of exercise was especially evident in the CF cohort, which developed dense network connections between SF metabolites and subchondral bone structural features.

Overall, we observed a consistent relationship between subchondral bone mineral density and SF metabolites in all groups except the HF sedentary condition. Moreover, a common set of annotated and unannotated SF metabolites were linked to joint structure or systemic factor variables in all diet and physical activity conditions, suggesting that a common set of metabolic pathways modulate joint homeostasis. SF metabolite features associated with joint homeostasis largely mapped to three classes of metabolites: 1) branched chain amino acids (i.e., leucine, isoleucine, and valine) and short-chain fatty acid metabolism, 2) phosphatidylglycerols and phosphatidylcholines, and 3) diacylglycerols and triacylglycerols (Fig. 7).

SF branched chain amino acids and short-chain fatty acids were positively associated with tibial subchondral and trabecular bone features in the exercise cohorts. These two classes of metabolites regulate skeletal homeostasis through multiple mechanisms. For example, leucine activates the mechanistic target of rapamycin complex 1 (mTORC1) pathway[41], thereby increasing bone mass by stimulating osteoblast differentiation and activity[42] and inhibiting osteoclastogenesis[43]. In addition, beta-amino-isobutyric acid, a side product of valine catabolism, is produced by skeletal muscle during exercise and exerts numerous endocrine-like beneficial effects of exercise[44], including protecting osteocyte function[45]. Short chain fatty acids also promote bone mass by regulating osteoclast function[46]. We found that the short chain fatty acid propanoate was elevated in the SF of sedentary HF animals, whereas exercise reduced propanoate and another short-chain fatty acid, butanoate.

Propanoate and butanoate downregulate osteoclast genes, such as TRAF6 and NFATc1, by shifting osteoclast metabolism toward glycolysis[46]. These short chain fatty acids are largely produced by fermentation activity of specific gut bacterial species[47], which may be relevant to OA risk[48]. In total, our findings indicate numerous potential mechanisms of action between the SF metabolome and subchondral bone remodeling.

Prior metabolomic studies have identified several metabolic biomarkers of OA, including phosphatidylcholines and the ratio of serum branched chain amino acids to histidine[16,49]. For example, SF concentrations of unsaturated phosphatidylcholines are reduced in OA patients undergoing joint replacement compared to controls[49]. We observed numerous negative associations of SF phosphatidylcholines with serum biomarkers of insulin sensitivity and positive associations with inflammation and joint adiposity. Diet and activity also altered SF branched chain amino acids. Given this evidence, adjusting for diet and activity may be necessary to establish predictive metabolic biomarkers of OA onset and progression.

We used correlation-based network analyses to integrate disparate phenotypic data that spanned from the whole organism to metabolites. This approach revealed differences across HF diet and exercise treatments that went largely undetected using standard comparisons of mean differences. Notably, exercise greatly increased connections between joint structural features and the SF metabolome. Bone features were the primary joint structure variables that established dense network modules with SF metabolites. It is not clear if other structural components, such as synovium or cartilage, were more minor contributors because they are less metabolically active, contribute less to the total joint tissue volume, or involved specific structural features that were less related to changes in metabolism.

In addition, modest levels of voluntary exercise were sufficient to disrupt SF metabolome links with serum glucose intolerance and inflammation and instead establish links to the anti-inflammatory cytokine IL-10 and subchondral bone in HF diet-induced obese mice. These findings are of interest based on the potential involvement of IL-10 in OA[50]. In a lipodystrophic mouse model that lacks fat pads throughout the body and is protected from post-traumatic OA, serum levels of IL-10 were greatly elevated relative to wild-type controls and were negatively associated with OA pathology[51]. We found that serum IL-10 was negatively associated with several classes of SF fatty acids in the HF diet exercise cohort. Given the recent positive pre-clinical OA therapy outcomes involving intra-articular IL-10 gene transfer[52,53], it could be worth testing if the mechanism of action involves altering SF lipids.

When knee OA was specifically evaluated in the network models using Dijkstra’s algorithm, SF metabolites related to extracellular lipid transport contributed to the shortest path linking body weight to knee OA in HF diet and exercise cohorts. It is surprising that a measure of body fat only contributed to this path in the CF sedentary cohort. One potential explanation for this observation is that the variation in body fat and epididymal fat was substantially reduced in the HF diet cohorts compared to the CF diet cohorts (Table S6). Body fat could contribute to the overall increase in OA pathology in the HF diet cohorts through a threshold effect that would not be detected by correlation. A similar phenomenon could also apply to

other factors, which is a limitation of the correlation network model approach. Nevertheless, these exploratory network-based observations provide an intriguing framework for future mechanistic studies investigating extracellular lipid transport in OA pathology.

This exploratory study has a number of additional limitations. The use of only male mice limits our ability to generalize the results to females. In addition, the study involved numerous comparisons and was not powered *a priori* to detect statistically significant changes in systemic metabolic and inflammatory outcome measures reported in this study. Thus, these statistical analyses should be interpreted with caution. The cross-sectional nature of this study design prevents the evaluation of causality, especially for the analysis of SF metabolites where diet and disease co-vary. The extensive time and resources required to conduct this study also limited our ability to confirm results in a separate replication cohort, although our prior study similarly reported diet and activity-specific networks linking joint structure and metabolic phenotypes[30]. Another limitation is that global metabolomic profiling only putatively assigns metabolite identities. Future studies are required to replicate and validate the identified SF metabolic networks using targeted methods. A comparison between SF and serum metabolites would also provide valuable insight into the relationship between systemic and local metabolic variables. This comparison would also benefit from the use of agnostic serum marker analyses. Finally, function-based outcomes were only evaluated in a subset of animals and therefore were not included in the network analyses. Exercise is effective at reducing OA pain and improving function. Therefore, function and pain-related behavior outcomes should be included in future network studies to improve the clinical relevance.

In conclusion, voluntary exercise initiated after the development of diet-induced obesity in mice did not alter the severity of knee OA, either positively or negatively. This outcome is consistent with prior clinical studies showing that moderately increased physical activity in individuals with obesity and OA does not exacerbate radiographic OA[23,54]. However, a detailed correlation-based network analysis indicates that exercise may re-establish network features observed in control animals that were lost with a HF diet. Exercise also disrupted network links between SF metabolites and systemic glucose intolerance in obese mice without improving systemic glucose tolerance. These findings suggest that whole-body improvements in metabolic health may not be required for modest levels of physical activity to improve the metabolic health of joints.

Supplementary Material

Refer to Web version on PubMed Central for supplementary material.

Acknowledgements

The authors gratefully acknowledge the excellent contributions of Ms. Joanna Hudson (deceased), who participated in the study design, acquisition of data, and data analysis. We would like to acknowledge the Mass Spectrometry CORE at Montana State University for their expertise and assistance in mass spectrometry. We would also like to thank Dr. Erik Adams for providing clinical relevance and Dr. Mark Greenwood for his assistance with statistical analyses. We further thank Griffin Lab members Erin Hutchison, Melinda West, Graham Roach, Dr. Yao Fu, and Dr. Rachel Lane for their assistance with data collection, data analysis, and/or animal care. Finally, we acknowledge the OMRF Imaging Core Facility for assistance with tissue processing for histological evaluation.

Funding

Funding: Supported by the NIH (grants P20RR018758, P20GM103441, P30GM114731, R03AR066828, R01AG049058 to Dr. Griffin and R01AR073964 to Dr. June), the Arthritis Foundation (Arthritis Investigator Award to Dr. Griffin), the Department of Veterans Affairs (I01BX004666, 1I01BX004882 Merit Awards to Dr. Griffin) and the National Science Foundation (CMMI 1554708 to Dr. June). The content is solely the responsibility of the authors and does not necessarily represent the official views of the National Institutes of Health, the Arthritis Foundation, the Department of Veterans Affairs, or the National Science Foundation.

Abbreviations:

OA	osteoarthritis
HF	high-fat
CF	control-fat
SF	synovial fluid
Ex	exercise
Sed	sedentary
GTT	glucose tolerance test
AUC	area under the curve
LC-MS	liquid chromatography-mass spectrometry
m/z	mass-to-charge ratio
HCA	hierarchical cluster analysis.

References

1. Dobson GP, Letson HL, Grant A, et al. Defining the osteoarthritis patient: back to the future. Osteoarthritis Cartilage. 2018;26(8):1003–1007. doi:10.1016/j.joca.2018.04.018. [PubMed: 29775734]
2. Mueller AJ, Peffers MJ, Proctor CJ, Clegg PD. Systems approaches in osteoarthritis: Identifying routes to novel diagnostic and therapeutic strategies. J Orthop Res. 2017;35(8):1573–1588. doi:10.1002/jor.23563. [PubMed: 28318047]
3. Loeser RF, Goldring SR, Scanzello CR, Goldring MB. Osteoarthritis: A disease of the joint as an organ. Arthritis Rheum. 2012;64(6):1697–1707. doi:10.1002/art.34453. [PubMed: 22392533]
4. Issa RI, Griffin TM. Pathobiology of obesity and osteoarthritis: integrating biomechanics and inflammation. Pathobiology of Aging & Age-related Diseases. 2012;2(0). doi:10.3402/pba.v2i0.17470.
5. Berenbaum F, Griffin TM, Liu-Bryan R. Review: Metabolic Regulation of Inflammation in Osteoarthritis. Arthritis Rheumatol. 2017;69(1):9–21. doi:10.1002/art.39842. [PubMed: 27564539]
6. Visser AW, de Mutsert R, le Cessie S, et al. The relative contribution of mechanical stress and systemic processes in different types of osteoarthritis: The NEO study. Annals of the Rheumatic Diseases. 2015;74(10):1842–1847. doi:10.1136/annrheumdis-2013-205012. [PubMed: 24845389]
7. Menni C, Zierer J, Valdes AM, Spector TD. Mixing omics: Combining genetics and metabolomics to study rheumatic diseases. Nat Rev Rheumatol. 2017;13(3):174–181. doi:10.1038/nrrheum.2017.5. [PubMed: 28148918]

8. Zhai G, Randell EW, Rahman P. Metabolomics of osteoarthritis: Emerging novel markers and their potential clinical utility. Rheumatology (Oxford). 2018;57(12):2087–2095. doi:10.1093/rheumatology/kex497. [PubMed: 29373736]
9. Jaggard MKJ, Boulangé CL, Akhbari P, et al. A systematic review of the small molecule studies of osteoarthritis using nuclear magnetic resonance and mass spectroscopy. Osteoarthritis Cartilage. 2019;27(4):560–570. doi:10.1016/j.joca.2018.08.024. [PubMed: 30287397]
10. Jang C, Chen L, Rabinowitz JD. Metabolomics and Isotope Tracing. Cell. 2018;173(4):822–837. doi:10.1016/j.cell.2018.03.055. [PubMed: 29727671]
11. Carlson AK, Rawle RA, Adams E, Greenwood MC, Bothner B, June RK. Application of global metabolomic profiling of synovial fluid for osteoarthritis biomarkers. Biochemical and Biophysical Research Communications. 2018;499(2):182–188. doi:10.1016/j.bbrc.2018.03.117. [PubMed: 29551687]
12. Mickiewicz B, Kelly JJ, Ludwig TE, et al. Metabolic analysis of knee synovial fluid as a potential diagnostic approach for osteoarthritis. J Orthop Res. 2015;33(11):1631–1638. doi:10.1002/jor.22949. [PubMed: 26010167]
13. Zhang W, Likhodii S, Zhang Y, et al. Classification of osteoarthritis phenotypes by metabolomics analysis. BMJ Open. 2014;4(11):e006286. doi:10.1136/bmjopen-2014-006286.
14. Zheng K, Shen N, Chen H, et al. Global and targeted metabolomics of synovial fluid discovers special osteoarthritis metabolites. J Orthop Res. 2017;35(9):1973–1981. doi:10.1002/jor.23482. [PubMed: 28439964]
15. Adams SB Jr, Setton LA, Kensicki E, Bolognesi MP, Toth AP, Nettles DL. Global metabolic profiling of human osteoarthritic synovium. Osteoarthritis Cartilage. 2012;20(1):64–67. doi:10.1016/j.joca.2011.10.010. [PubMed: 22063369]
16. Zhai G, Wang-Sattler R, Hart DJ, et al. Serum branched-chain amino acid to histidine ratio: a novel metabolomic biomarker of knee osteoarthritis. Ann Rheum Dis. 2010;69(6):1227–1231. doi:10.1136/ard.2009.120857. [PubMed: 20388742]
17. Zhang W, Sun G, Likhodii S, et al. Metabolomic analysis of human plasma reveals that arginine is depleted in knee osteoarthritis patients. Osteoarthritis Cartilage. 2016;24(5):827–834. doi:10.1016/j.joca.2015.12.004. [PubMed: 26708258]
18. Lamers RJAN, van Nesselrooij JHJ, Kraus VB, et al. Identification of an urinary metabolite profile associated with osteoarthritis. Osteoarthritis Cartilage. 2005;13(9):762–768. doi:10.1016/j.joca.2005.04.005. [PubMed: 15951202]
19. Carlson AK, Rawle RA, Wallace CW, et al. Characterization of synovial fluid metabolomic phenotypes of cartilage morphological changes associated with osteoarthritis. Osteoarthritis Cartilage. 2019;27(8):1174–1184. doi:10.1016/j.joca.2019.04.007. [PubMed: 31028882]
20. Kim S, Hwang J, Kim J, Ahn JK, Cha H-S, Kim KH. Metabolite profiles of synovial fluid change with the radiographic severity of knee osteoarthritis. Joint Bone Spine. 2017;84(5):605–610. doi:10.1016/j.jbspin.2016.05.018. [PubMed: 27461192]
21. Zhang W, Likhodii S, Aref-Eshghi E, et al. Relationship between blood plasma and synovial fluid metabolite concentrations in patients with osteoarthritis. J Rheumatol. 2015;42(5):859–865. doi:10.3899/jrheum.141252. [PubMed: 25729031]
22. Fransen M, McConnell S, Harmer AR, Van der Esch M, Simic M, Bennell KL. Exercise for osteoarthritis of the knee. Cochrane Musculoskeletal Group, ed. Cochrane Database Syst Rev. 2015;1(2):CD004376. doi:10.1002/14651858.CD004376.pub3. [PubMed: 25569281]
23. Messier SP, Mihalko SL, Legault C, et al. Effects of Intensive Diet and Exercise on Knee Joint Loads, Inflammation, and Clinical Outcomes Among Overweight and Obese Adults With Knee Osteoarthritis: The IDEA Randomized Clinical Trial. JAMA. 2013;310(12):1263–1273. doi:10.1001/jama.2013.277669. [PubMed: 24065013]
24. Collins S, Martin TL, Surwit RS, Robidoux J. Genetic vulnerability to diet-induced obesity in the C57BL/6J mouse: physiological and molecular characteristics. Physiology & Behavior. 2004;81(2):243–248. doi:10.1016/j.physbeh.2004.02.006. [PubMed: 15159170]
25. Xu H, Barnes GT, Yang Q, et al. Chronic inflammation in fat plays a crucial role in the development of obesity-related insulin resistance. J Clin Invest. 2003;112(12):1821–1830. [PubMed: 14679177]

26. Griffin TM, Fermor B, Huebner JL, et al. Diet-induced obesity differentially regulates behavioral, biomechanical, and molecular risk factors for osteoarthritis in mice. Arthritis Res Ther. 2010;12(4):R130. doi:10.1186/ar3068. [PubMed: 20604941]
27. Griffin TM, Huebner JL, Kraus VB, Yan Z, Guilak F. Induction of osteoarthritis and metabolic inflammation by a very high-fat diet in mice: Effects of short-term exercise. Arthritis Rheum. 2012;64(2):443–453. doi:10.1002/art.33332. [PubMed: 21953366]
28. Barboza E, Hudson J, Chang W-P, et al. Profibrotic Infrapatellar Fat Pad Remodeling Without M1 Macrophage Polarization Precedes Knee Osteoarthritis in Mice With Diet-Induced Obesity. Arthritis & Rheumatology. 2017;69(6):1221–1232. doi:10.1002/art.40056. [PubMed: 28141918]
29. Donovan EL, Lopes EBP, Batushansky A, Kinter M, Griffin TM. Independent effects of dietary fat and sucrose content on chondrocyte metabolism and osteoarthritis pathology in mice. Dis Model Mech. 2018;11(9):dmm034827. doi:10.1242/dmm.034827. [PubMed: 30018076]
30. Griffin TM, Batushansky A, Hudson J, Lopes EBP. Correlation network analysis shows divergent effects of a long-term, high-fat diet and exercise on early stage osteoarthritis phenotypes in mice. J Sport Health Sci. 2020;9(2):119–131. doi:10.1016/j.jshs.2019.05.008. [PubMed: 32099720]
31. Griffin TM, Huebner JL, Kraus VB, Guilak F. Extreme obesity due to impaired leptin signaling in mice does not cause knee osteoarthritis. Arthritis Rheum. 2009;60(10):2935–2944. doi:10.1002/art.24854. [PubMed: 19790050]
32. Seifer DR, Furman BD, Guilak F, Olson SA, Brooks SC III, Kraus VB. Novel synovial fluid recovery method allows for quantification of a marker of arthritis in mice. Osteoarthritis Cartilage. 2008;16(12):1532–1538. doi:10.1016/j.joca.2008.04.013. [PubMed: 18538588]
33. Pluskal T, Castillo S, Villar-Briones A, Oresic M. MZmine 2: modular framework for processing, visualizing, and analyzing mass spectrometry-based molecular profile data. BMC Bioinformatics. 2010;11:395. doi:10.1186/1471-2105-11-395. [PubMed: 20650010]
34. Chong J, Soufan O, Li C, et al. MetaboAnalyst 4.0: towards more transparent and integrative metabolomics analysis. Nucleic Acids Res. 2018;46(W1):W486–W494. doi:10.1093/nar/gky310. [PubMed: 29762782]
35. Guijas C, Montenegro-Burke JR, Domingo-Almenara X, et al. METLIN: A Technology Platform for Identifying Knowns and Unknowns. Anal Chem. 2018;90(5):3156–3164. doi:10.1021/acs.analchem.7b04424. [PubMed: 29381867]
36. Li S, Park Y, Duraisingham S, et al. Predicting network activity from high throughput metabolomics. PLoS Comput Biol. 2013;9(7):e1003123. doi:10.1371/journal.pcbi.1003123. [PubMed: 23861661]
37. Batushansky A, Toubiana D, Fait A. Correlation-Based Network Generation, Visualization, and Analysis as a Powerful Tool in Biological Studies: A Case Study in Cancer Cell Metabolism. BioMed Research International. 2016;2016:8313272. doi:10.1155/2016/8313272. [PubMed: 27840831]
38. Revelle WR (Photographer), psych : Procedures for Personality and Psychological Research.
39. Shannon P, Markiel A, Ozier O, et al. Cytoscape: a software environment for integrated models of biomolecular interaction networks. Genome Res. 2003;13(11):2498–2504. doi:10.1101/gr.1239303. [PubMed: 14597658]
40. Csárdi G, Nepusz T. The igraph software package for complex network research. In:; 2006.
41. Goberdhan DCI, Wilson C, Harris AL. Amino Acid Sensing by mTORC1: Intracellular Transporters Mark the Spot. Cell Metab. 2016;23(4):580–589. doi:10.1016/j.cmet.2016.03.013. [PubMed: 27076075]
42. Chen J, Long F. mTOR signaling in skeletal development and disease. Bone Res. 2018;6(1):1. doi:10.1038/s41413-017-0004-5. [PubMed: 29423330]
43. Ozaki K, Yamada T, Horie T, et al. The L-type amino acid transporter LAT1 inhibits osteoclastogenesis and maintains bone homeostasis through the mTORC1 pathway. Science Signaling. 2019;12(589). doi:10.1126/scisignal.aaw3921.
44. Roberts LD, Bostrom P, O'Sullivan JF, et al. β-Aminoisobutyric acid induces browning of white fat and hepatic β-oxidation and is inversely correlated with cardiometabolic risk factors. Cell Metab. 2014;19(1):96–108. doi:10.1016/j.cmet.2013.12.003. [PubMed: 24411942]

45. Kitase Y, Vallejo JA, Gutheil W, et al. β-aminoisobutyric Acid, l-BAIBA, Is a Muscle-Derived Osteocyte Survival Factor. CellReports. 2018;22(6):1531–1544. doi:10.1016/j.celrep.2018.01.041.

46. Lucas S, Omata Y, Hofmann J, et al. Short-chain fatty acids regulate systemic bone mass and protect from pathological bone loss. Nat Comms. 2018;9(1):55. doi:10.1038/s41467-017-02490-4.

47. Koh A, De Vadder F, Kovatcheva-Datchary P, Bäckhed F. From Dietary Fiber to Host Physiology: Short-Chain Fatty Acids as Key Bacterial Metabolites. Cell. 2016;165(6):1332–1345. doi:10.1016/j.cell.2016.05.041. [PubMed: 27259147]

48. Favazzo LJ, Hendesi H, Villani DA, et al. The gut microbiome-joint connection: implications in osteoarthritis. Curr Opin Rheumatol. 2020;32(1):92–101. doi:10.1097/BOR.0000000000000681. [PubMed: 31724973]

49. Zhang W, Sun G, Likhodii S, et al. Metabolomic analysis of human synovial fluid and plasma reveals that phosphatidylcholine metabolism is associated with both osteoarthritis and diabetes mellitus. Metabolomics. 2016;12(2):24.

50. Barker T, Rogers VE, Henriksen VT, Trawick RH, Momberger NG, Rasmussen GL. Circulating IL-10 is compromised in patients predisposed to developing and in patients with severe knee osteoarthritis. Sci Rep-uk. 2021;11(1):1812. doi:10.1038/s41598-021-81382-6

51. Collins KH, Lenz KL, Pollitt EN, et al. Adipose tissue is a critical regulator of osteoarthritis. Proc National Acad Sci. 2021;118(1):e2021096118. doi:10.1073/pnas.2021096118

52. Moss KL, Jiang Z, Dodson ME, et al. Sustained Interleukin-10 Transgene Expression Following Intra-Articular AAV5-IL-10 Administration to Horses. Hum Gene Ther. 2020;31 (1-2):110–118. doi:10.1089/hum.2019.195 [PubMed: 31773987]

53. Watkins LR, Chavez RA, Landry R, et al. Targeted interleukin-10 plasmid DNA therapy in the treatment of osteoarthritis: Toxicology and pain efficacy assessments. Brain Behav Immun. 2020;90:155–166. doi:10.1016/j.bbi.2020.08.005 [PubMed: 32800926]

54. Felson DT, Niu J, Clancy M, Sack B, Aliabadi P, Zhang Y. Effect of recreational physical activities on the development of knee osteoarthritis in older adults of different weights: the Framingham Study. Arthritis Rheum. 2007;57(1):6–12. doi:10.1002/art.22464. [PubMed: 17266077]

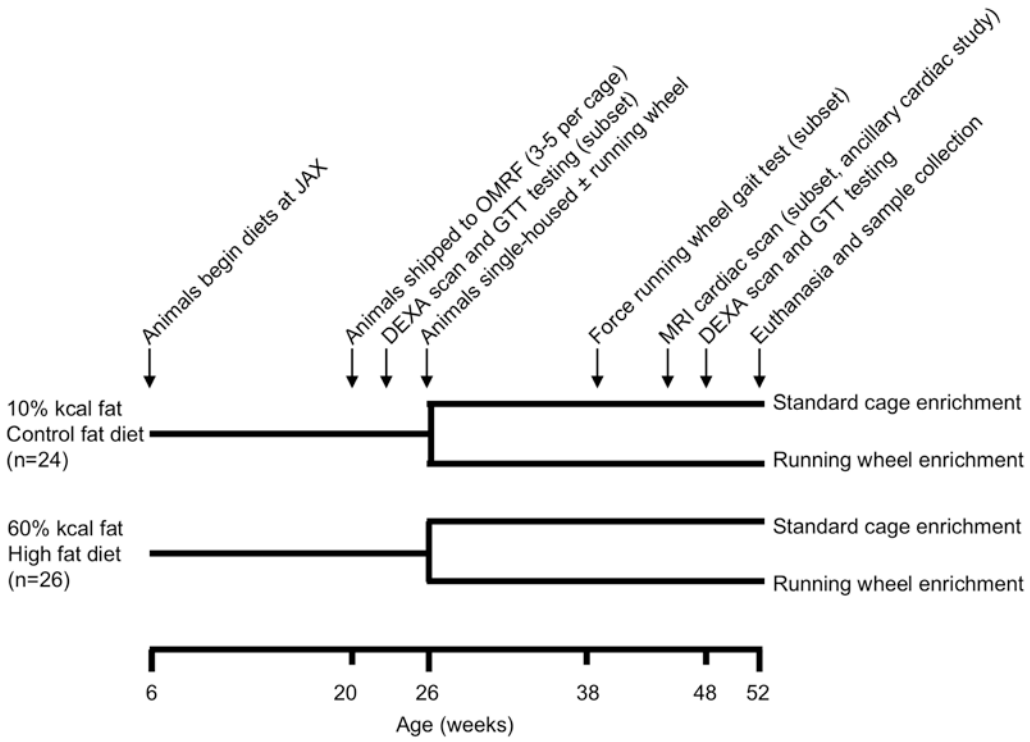

Figure 1. Timeline of experimental procedures.

Male C57BL/6J mice were purchased from The Jackson Laboratory (JAX) through the Diet-Induced Obese Mouse service, which assigns animals to one of two irradiated, purified open-source diets (Research Diets Inc.) beginning at 6 weeks of age: 1) control-fat diet (CF) containing 10% kcal fat (D12450Bi), or 2) high-fat diet (HF) containing 60% kcal fat (D12492i). 3 animals assigned to the exercise cohort in each diet and one HF-sedentary animal died during the course of the experiment due to undetermined causes, resulting in the following final group sizes: CF-sedentary (n=12), CF-exercise (n=9), HF-sedentary (n=13), HF-exercise (n=9). Abbreviations: OMRF (Oklahoma Medical Research Foundation), DEXA (dual X-ray absorptiometry system), GTT (glucose tolerance testing), and MRI (magnetic resonance imaging).

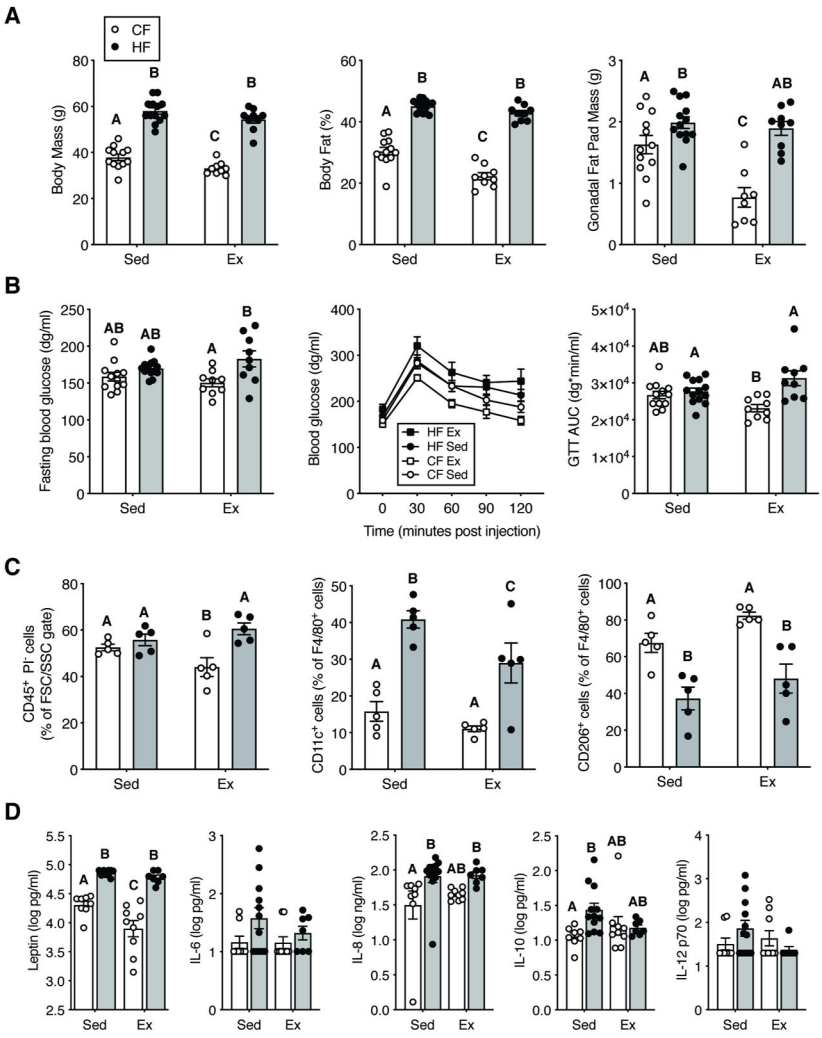

Figure 2. Effect of HF diet and exercise on systemic markers of metabolism and inflammation.

A. HF diet increased body mass and percent body fat compared to CF sedentary animals. Exercise in CF animals reduced percent body fat and gonadal fat mass. B. In animals given wheel access, fasting blood glucose was elevated by a HF diet, but diet did not alter fasting blood glucose in sedentary animals. Exercise improved glucose tolerance in CF diet mice relative to HF diet mice as indicated by reduced glucose area under the curve (AUC). C. Gonadal fat pad stromal vascular fraction immune cells. Exercise in CF diet animals reduced adipose immune cells. HF diet increased fat inflammation by decreasing M2-like F4/80+, CD206+ cells and increasing M1-like F4/80+, CD11c+ cells. Exercise modestly reduced M1-like cells in HF diet mice. D. Serum adipokine, chemokine, and cytokine concentrations collected at the termination of the study. HF diet increased serum markers of leptin, IL-8, and IL-10, although exercise also altered leptin and IL-10. Bars = mean+/−sem. Bars not connected by the same letter are significantly different (Fisher's LSD post-hoc test following $p<0.05$ 2-Factor ANOVA).

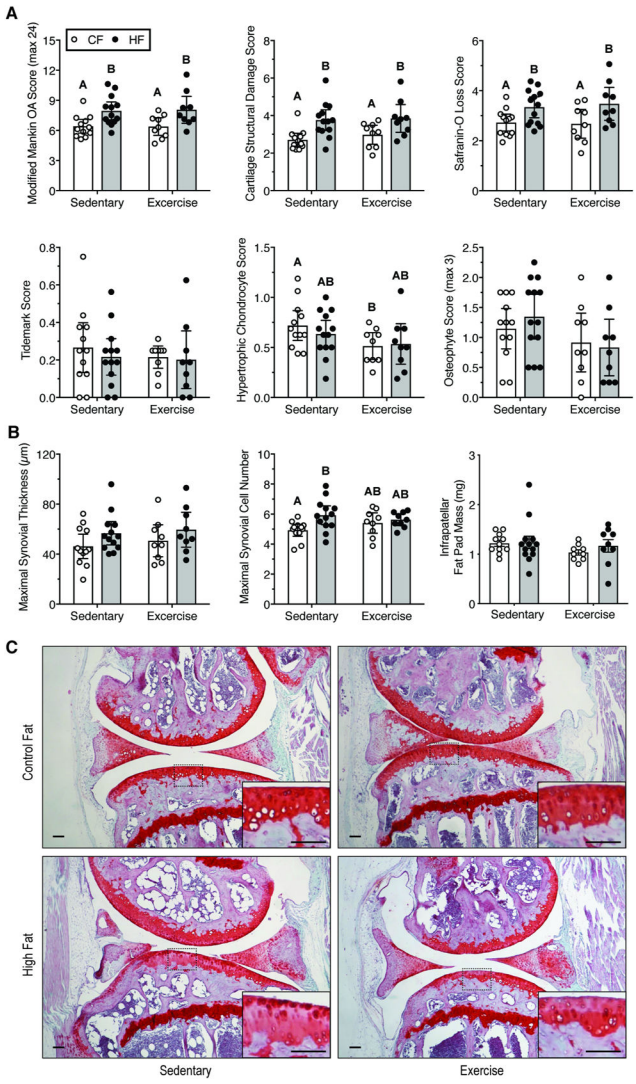

Figure 3. Effect of HF diet and voluntary wheel running on knee OA pathology.

A. Semi-quantitative OA histopathology scores. Scoring was conducted by two blinded graders throughout the joint (medial and lateral, tibia and femur). Modified Mankin scoring is the summation of cartilage damage, safranin-O loss, tidemark duplication, and hypertrophic chondrocyte scores. Data points are values for individual animals, and bars are mean +/− 95% CI. Significant differences between groups are indicated by bars that do not share a common letter (2-factor ANOVA, $p<0.05$, followed by Fisher's LSD post-hoc, $p<0.05$). B. Quantitative synovial thickness, cell layer number, and infrapatellar fat pad mass as biomarkers of joint inflammation (mean +/− 95% CI; statistical analyses as in panel A). C. Representative histological sagittal images from the medial compartment. Inset shows a magnified view of the tibial plateau as indicated by dashed rectangle. Scale bars are 100 μm.

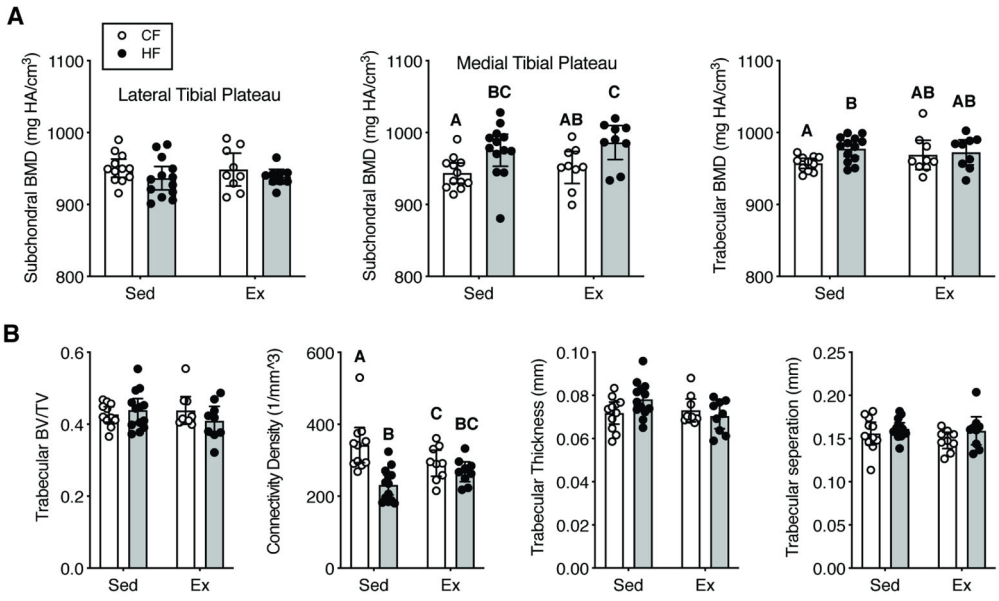

Figure 4. Effect of HF diet and voluntary wheel running on proximal tibia subchondral and trabecular bone density and morphology as measured by micro-CT.

A. Trabecular and medial compartment subchondral bone mineral density (BMD) was increased by a HF diet, especially in sedentary mice. B. Trabecular bone morphology was largely unaffected by a HF diet and voluntary wheel running. An exception was the trabecular connectivity density, which was reduced by a HF diet in sedentary but not exercise mice. BV=bone volume, TV=total volume. Data points are values for individual animals, and bars are mean +/− 95% CI. Significant differences between groups are indicated by bars that do not share a common letter (2-factor ANOVA, $p \leq 0.05$, followed by Fisher's LSD post-hoc, $p < 0.05$).

A

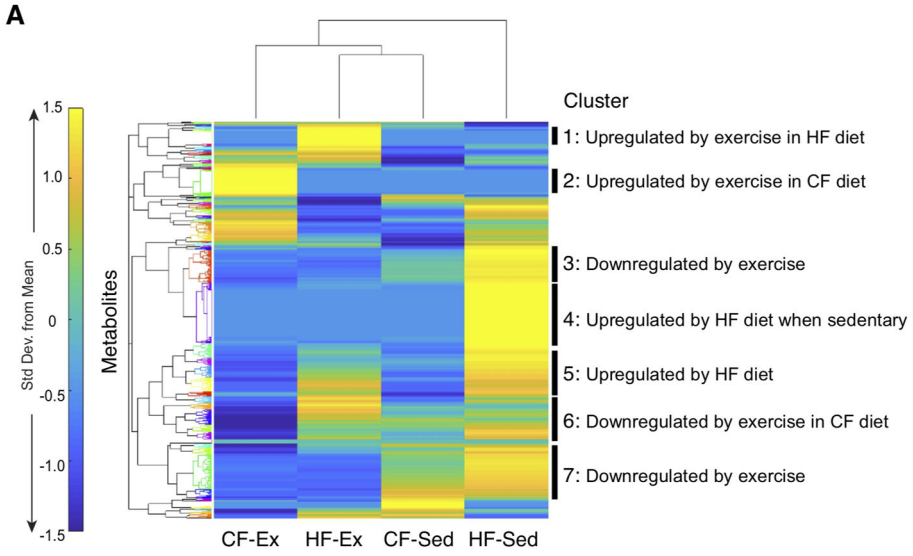

B

Cluster #	Select Enriched Metabolic Pathways (KEGG)
1	Pyrimidine metabolism, steroid hormone biosynthesis, glycolysis or gluconeogenesis, TCA cycle fructose and mannose metabolism
2	Steroid biosynthesis, primary bile acid biosynthesis, ubiquinone and other terpenoid-quinone biosynthesis, steroid hormone biosynthesis, tyrosine metabolism
3	Fatty acid metabolism/biosynthesis*, pyruvate metabolism*, tryptophan metabolism*, beta-alanine metabolism*, butanoate metabolism*, propanoate metabolism*, lysine degradation*
4	Propanoate metabolism*, beta-alanine metabolism*, pantothenate and CoA biosynthesis*, synthesis and degradation of ketone bodies*, valine, leucine, and isoleucine degradation*, terpenoid backbone biosynthesis*, TCA cycle*, tryptophan metabolism*, lysine degradation*, aminoacyl-tRNA biosynthesis*, butanoate metabolism*
5	TCA cycle*
6	Aminoacyl-tRNA biosynthesis, pentose phosphate pathway, pentose and glucuronate interconversions, steroid biosynthesis, steroid hormone biosynthesis
7	Tryptophan metabolism*, steroid biosynthesis*, lysine degradation*

Figure 5. Effect of diet and activity on global metabolomic features in mouse synovial fluid (SF).

A. Heatmap cluster-gram visualization of unsupervised hierarchical cluster analysis (HCA) based on median intensities for all 1412 detected metabolite features. HCA revealed that the most similar synovial fluid metabolomic profiles are from CF-Sed and HF-Ex mice. HF-Sed mouse synovial fluid had the most distinct metabolomic profile. Clusters of co-regulated metabolites were selected for pathway analysis based on a minimal number of metabolite features and observable separation by Euclidean distance. B. Metabolic pathways for each cluster were evaluated by MS Peaks to Pathway, which employs Mummichog. Pathways with an *a priori* significance level of q_{FDR}=0.05 are indicated by an asterisk. If no significant pathways were identified, the top five pathways were reported. A full enrichment analysis for heatmap clusters is reported in Supplemental Table S2.

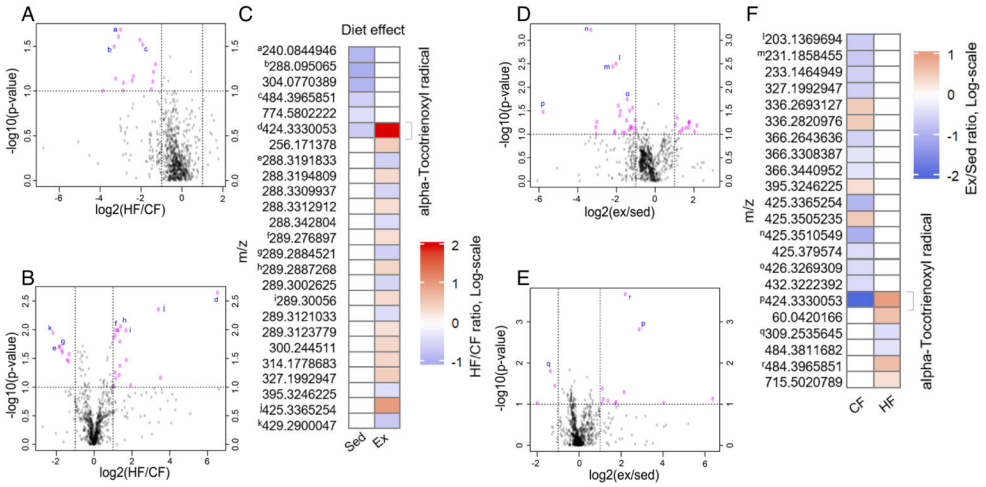

Figure 6. HF diet and wheel running interact to regulate synovial fluid metabolites.

A. Volcano plot of differentially expressed metabolite features between sedentary HF and CF cohorts. Log2(HF/CF) plotted against −log10(FDR-corrected Student's T-test p-value) to illustrate both significance and magnitude of change. Vertical dashed lines indicate 2-fold change and horizontal lines indicate $P_{FDR}<0.1$. B. Volcano plot of differentially expressed metabolite features between Exercise HF and CF cohorts. C. Heatmap of mean metabolite levels showing significantly up (red) or down (blue) regulated metabolites due to HF ($p<0.05$). Annotated metabolite derived from the Human Metabolome Database. D. Volcano plot of differentially expressed metabolite features between CF Exercise and sedentary cohorts. E. Volcano plot of differentially expressed metabolite features between HF Exercise and sedentary cohorts. F. Heatmap showing significantly up (red) or down (blue) regulated metabolites due to exercise ($p<0.05$). Superscript letters indicate identical metabolites between volcano plots and heatmaps.

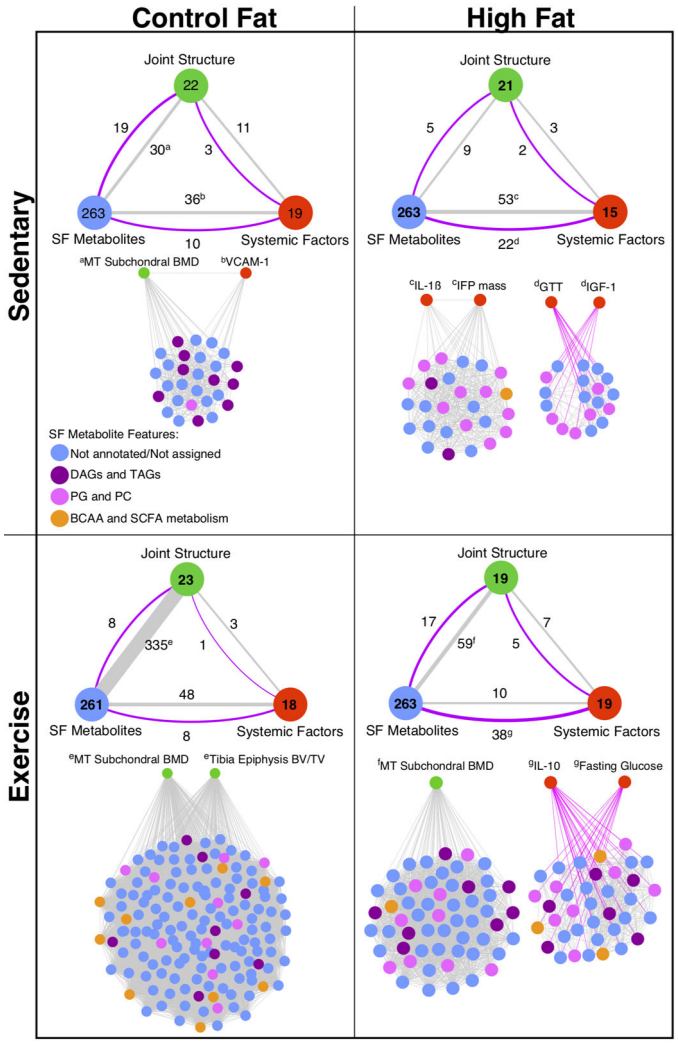

Figure 7. Correlation-based network analysis models.

Network models show distinct effects of HF diet and voluntary wheel running exercise on connectivity between systemic and local metabolic factors on joint structure. To help with interpreting the overall network for each diet and activity experimental group (Figure S5), network variables were categorized into one of three sub-group nodes: Joint Structure, SF Metabolites, or Systemic Factors. The number of variables with ≥1 significant correlations ($r>|\pm0.5|$ and qFDR<0.05) are shown in the large circles for each designated sub-group node of network variables, which are provided in Table S3. The number of correlated pairs of variables connecting the sub-groups are shown adjacent to the lines, whose thickness was proportional to the positive correlations (grey lines) and negative correlations (purple lines). Superscript letters indicate the primary network modules linking the indicated sub-groups to SF metabolites. Unabridged networks for each diet and activity group are shown in Figure S5. DAG: diacylglycerols; TAGs: triacylglycerols; PG: phosphatidylglycerol; PC: phosphatidylcholine; BCAA: branched chain amino acids; SCFA: short chain fatty acids.

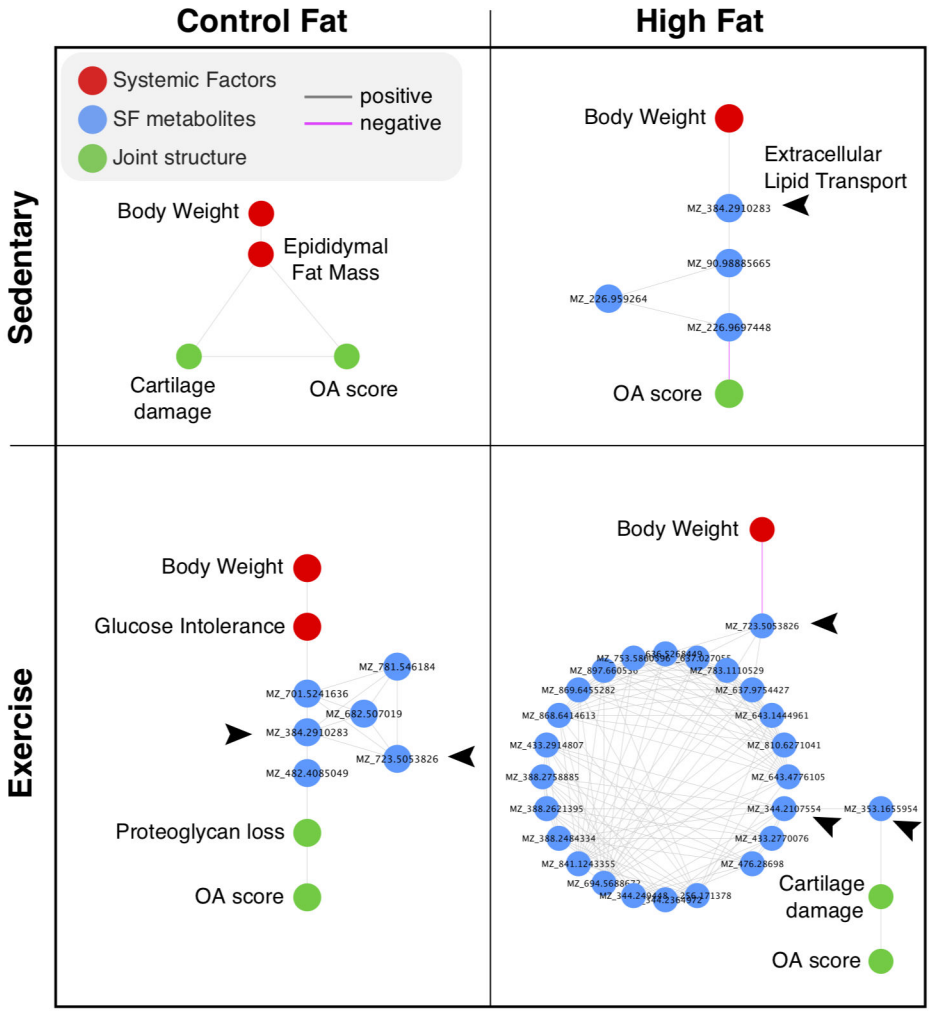

Figure 8. Correlation network shortest path results linking body weight to the modified Mankin whole-joint knee OA score.

|r|-values were used to estimate edge weights and transformed to a distance matrix for Dijkstra's shortest path algorithm. The algorithm was applied to the full network (Figure S5) to identify the network variables ("nodes") that most closely link body weight to knee OA across each diet and physical activity condition. Note that all diet and activity conditions, except for the CF sedentary group, involved synovial fluid (SF) metabolites in the shortest path. A tentative annotation of the metabolites based on m/z values indicates an enrichment for metabolites involved in extracellular lipid transport, as indicated by arrow heads. The glucose intolerance node refers to the glucose area under the curve value following a glucose tolerance test. Cartilage damage refers to this specific sub-component score of the modified Mankin OA score. Proteoglycan loss refers to the Safranin-0 stain loss sub-component score of the modified Mankin OA score.